Improving magnetic resonance spectroscopy in the brainstem periaqueductal grey using spectral registration

Laura Sirucek[1,2], Niklaus Zoelch[3,4], Petra Schweinhardt[1]

[1]*Department of Chiropractic Medicine, Integrative Spinal Research Group, Balgrist University Hospital, University of Zurich, Zurich, Switzerland*
[2]*Neuroscience Center Zurich, University of Zurich, Zurich, Switzerland*
[3]*Department of Forensic Medicine and Imaging, Institute of Forensic Medicine, University of Zurich, Zurich, Switzerland*
[4]*Department of Psychiatry, Psychotherapy and Psychosomatics, Psychiatric University Hospital Zurich, University of Zurich, Zurich, Switzerland*

Submitted to Magnetic Resonance in Medicine

Corresponding author
Laura Sirucek
Integrative Spinal Research
Balgrist Campus
Lengghalde 5
8008 Zurich
Switzerland
Phone: +41 44 510 7352
laura.sirucek@balgrist.ch
https://www.balgrist.ch/en/research/research-units/research-chiropractic/

Word count: 2800

Keywords: magnetic resonance spectroscopy, brainstem, postprocessing, small volume, head motion, relaxation time

Abstract

Purpose: Functional understanding of the periaqueductal grey (PAG), a physiologically and clinically highly relevant brainstem region, can be advanced using proton magnetic resonance spectroscopy (^{1}H-MRS). However, the PAG's small size and high levels of physiological noise are methodologically challenging. This study aimed to (1) improve ^{1}H-MRS data quality in the PAG using spectral registration for frequency and phase error correction, (2) investigate whether spectral registration is particularly useful in cases of greater head motion and (3) examine two metabolite quantification approaches using literature-based or individual-based water relaxation times.

Methods: Spectra were acquired in 33 healthy volunteers (50.1 years, SD=17.19, 18 females) on a 3T Philipps MR system using a point-resolved spectroscopy sequence optimized with very selective saturation pulses (OVERPRESS) and voxel-based flip angle calibration (effective volume of interest size: 8.8x10.2x12.2 mm^{3}).

Results: Spectral registration significantly improved signal-to-noise ratios (SNR; p=0.048, median value [interquartile range]: 18.0 [17.00-20.00]) and spectral linewidth (N-acetylaspartate peak: p<0.001, 4.3 Hz [3.96-4.85]), as well as metabolite fit (p's<0.046) compared to post-processing with minimal frequency alignment using interleaved unsuppressed water peaks. Correlational analyses revealed smaller improvements in SNR in cases of greater head motion (p=0.002) recorded with a markerless motion tracking system. Metabolite concentrations were higher when quantified using individual-based compared to literature-based water relaxation times (p's<0.001).

Conclusion: This study demonstrates that high-quality ^{1}H-MRS can be acquired in the PAG using spectral registration. This offers new opportunities for future ^{1}H-MRS studies in the PAG and possibly also other clinically relevant brain regions with similar methodological challenges.

Keywords: magnetic resonance spectroscopy, brainstem, postprocessing, small volume, head motion, relaxation time

1. Introduction

The periaqueductal grey (PAG) is a brainstem region with multiple pivotal functions for the human organism including the coordination of cardiovascular, respiratory, motor, and pain modulatory reactions to stress.[1] Various pathological conditions present with changes in PAG function. For instance, altered PAG functional connectivity has been observed in neurodegenerative diseases,[2,3] migraine,[4,5] headache,[6] fibromyalgia,[7-9] neuropathic pain,[10] and chronic low back pain.[11] A more complete understanding of PAG function in health and disease can be gained by examining the PAG's neurochemical properties. Proton MR spectroscopy (^{1}H-MRS) offers a non-invasive method to obtain in vivo neurochemical information about human brain tissue.

In the PAG, ^{1}H-MRS has been investigated in patients with chronic migraine,[12,13] chronic daily headaches,[14] and chronic whiplash injury.[15] Yet, the number of ^{1}H-MRS studies in the PAG is limited, which may be due to several difficulties associated with ^{1}H-MRS acquisition in this region: first, the PAG is a small structure of approximately 4-5 mm diameter and 14 mm length,[16] i.e. approximately 5x5x14 mm^3 (APxLRxFH). Second, the PAG is prone to physiological noise due to its proximity to pulsating anatomical structures, such as major arteries and cerebrospinal fluid (CSF)-filled spaces.[17] The existing PAG ^{1}H-MRS studies employed different approaches to address these challenges. Lai and colleagues[12] used a long echo time (TE) of 144 ms, which produces a better baseline and allows a more stable detection of the main metabolites creatine (Cre), choline (Cho), and N-acetylaspartate (NAA).[18] However, various neurobiologically relevant metabolites, e.g. myo-inositol (mI) or glutamate (Glu), require shorter TEs to be detected. Another option is to sacrifice regional specificity by using volume of interest (VOI) sizes lager than the PAG itself, e.g. 20x20x20 mm^3,[13,14] because the signal to noise ratio (SNR) increases proportionally to VOI size.[19] Smaller VOIs require longer acquisition times to achieve sufficient SNR, which might in turn impair the spectral quality because of increasing frequency drifts over time and a higher risk for head motion inducing additional frequency and phase errors.[20,21] A promising tool to address the problem of frequency and phase drifts or errors is offered by advanced post-processing techniques such as spectral registration.[20]

In this study, the aim was to record high-quality ^{1}H-MR spectra in a 8.8x10.2x12.2 mm^3 VOI covering the PAG of healthy volunteers using a point-resolved spectroscopy sequence (PRESS)[22,23] optimized with very selective saturation pulses (OVERPRESS)[24-26] and voxel-based flip angle calibration[27,28] combined with spectral registration.[20] The spectral quality was compared to the spectral quality achieved with minimal frequency alignment, i.e. using the unsuppressed water peak of multiple interleaved spectra. In addition, it was investigated whether spectral registration was particularly useful in cases of greater head motion measured

with a markerless motion tracking system.[29] Lastly, because tissue-specific water T_1 and T_2 relaxation times vary across different brain regions[30-32] and standard literature-based values might not generalize to the PAG, differences in metabolite concentrations using literature-based or individual-based water relaxation times were examined. The data presented in this manuscript are part of a larger study investigating differences in PAG spectra between pain-free volunteers and patients with chronic low back pain.

2. Methods

2.1 Participants

Thirty-four healthy volunteers were recruited via online advertisements and oral communication. The participants were age- and sex-matched to a cohort of patients with chronic low back pain as part of a larger study (Clinical Research Priority Program "Pain", https://www.crpp-pain.uzh.ch/en.html). The data of the patient cohort is not part of the present research question and are therefore not discussed. Inclusion criteria were over 18 and below 80 years of age, good general health and free of low back pain lasting longer than 3 consecutive days during the last year. Exclusion criteria comprised any major medical or psychiatric condition, pregnancy, inability to follow study instructions and any contraindication to MR imaging. The study was approved by the local ethics committee "Kantonale Ethikkommission Zürich" (Nr.: 2019-00136, clinicaltrials.gov: NCT04433299) and was performed according to the guidelines of the Declaration of Helsinki (2013). Written informed consent was obtained from all participants before the start of the experiment.

2.2 Study Design Overview

The larger study comprised three experimental sessions of approximately 3 hours each. The first two sessions included a clinical examination as well as neurophysiological and psychophysical assessments. During the third session, participants underwent two MR measurements, one ^{1}H-MRS scan and one resting state functional MR imaging scan with a break of one hour in between. All scans were performed after 12 pm. Only the ^{1}H-MRS data are subject of the present study.

2.3 Magnetic resonance spectroscopy

Technical details of the ^{1}H-MRS acquisition, post-processing and metabolite quantification are listed in Table S1. The following sections provide a brief overview of the applied methods.

2.3.1 Acquisition

^{1}H-MRS was acquired on a 3T MR system using a 32-channel receive-only phased-array head coil (Philips Healthcare, Best, The Netherlands). Prior to ^{1}H-MRS acquisition, high-resolution (1 mm^3 isotropic) anatomical T_1-weighted images were obtained. Based on the 3D T_1 images, the VOI was placed to cover the PAG according to anatomical landmarks by the same examiner (LS) for all participants (Figure 1). Spectra were localized using a water-suppressed single-voxel PRESS sequence[22,23] (repetition time (TR): 2500 ms, TE: 33 ms, number of signals averaged: 512 divided into 8 blocks of 64) optimized with six very selective saturation (VSS) pulses (OVERPRESS)[24-26] to minimize errors in chemical-shift displacement and to achieve consistent localization volumes across all metabolites of interest (Figure 1), and with voxel-based flip angle calibration[27,28] to achieve an optimal flip angle within the VOI. Accounting for the VSS pulses, the resulting VOI size was 8.8x10.2x12.2 mm^3=1.1 mL. For each individual, two water signals were acquired: one for eddy-current correction and literature-based water referencing obtained from interleaved water unsuppressed spectra (one before each of the 8 blocks) during the ^{1}H-MRS acquisition in the PAG (WR-shortTR) and one for an individual-based water referencing approach (see 2.3.3 Metabolite quantification), where a fully-relaxed water signal was estimated from a separate water reference scan after the ^{1}H-MRS acquisition in the PAG within the same VOI with a TR of 10000 ms (WR-longTR). The 3D T_1 and ^{1}H-MRS acquisition in the PAG took 7 min 32 s and 23 min 20 s, respectively.

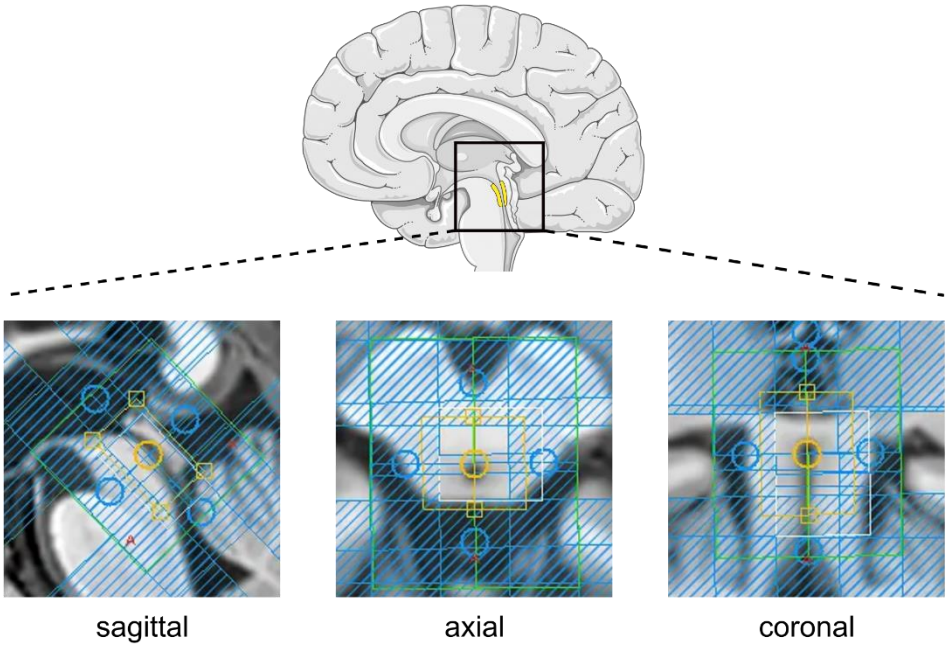

Figure 1. Volume of interest (VOI) placement over the brainstem periaqueductal grey (PAG). The yellow box depicts the VOI's nominal size (11x15x18 mm^3 [APxLRxFH]. The

blue-shaded areas depict the six very selective saturation (VSS) bands used to minimize errors in chemical-shift displacement and to achieve consistent localization volumes across all metabolites of interest. The unshaded area within the yellow box depicts the final VOI size (8.8x10.2x12.2 mm^3) accounting for the VSS bands.

2.3.2 Post-processing

For the approach *with spectral registration,* frequency alignment was performed using spectral registration in the time domain (adopted from[20,33]). For that, the data was 8-fold zero-filled and filtered with a 2 Hz Gaussian filter. Only the first 500 ms were used for alignment and the single averages were aligned to the median of all averages. *Without spectral registration*, minimal frequency alignment was achieved by eddy-current correction,[34] i.e. eddy-current correcting the 64 averages of each block using the unsuppressed water scan (WR-shortTR) acquired prior to the respective block.

For both approaches, the post-processed spectra were visually checked for artefacts. Spectra with artefacts were excluded from further analyses, as well as spectra presenting with insufficient quality,[28] i.e. with a full width at half maximum (FWHM) value of the unsuppressed water peak (FWHM H_2O; shim quality indicator) above 2.5 median absolute deviation (MAD)[35] of the group median or with a signal-to-noise ratio (SNR) below 2.5 MAD of the group median.

2.3.3 Metabolite quantification

All spectra were analyzed using LCModel (6.3).[36] Metabolite concentrations are reported as ratios to the unsuppressed water signal and reflect an estimation of metabolite concentration in moles per kg of tissue water excluding water within CSF. The fully relaxed water signal was estimated in two ways: (1) literature-based, i.e. using the unsuppressed water signal from the WR-shortTR scans and literature values to correct relaxation attenuation. And (2), individual-based, using the TE series acquired with the WR-longTR scan. Varying TEs allow to estimate the T_2 relaxation time of water within the VOI and therewith, to obtain a subject-specific approximation of the fully-relaxed water signal.[37] Next to being independent of literature-based tissue-specific T_1 and T_2 relaxation times, this approach is also less reliant on correct segmentation of grey matter (GM), white matter (WM) and CSF compared to the literature-based approach.

2.3.4 Motion tracking

Head motion was measured in 25 participants using the markerless motion tracking system Tracoline TCL3 with the TracSuite software 3.1.9 (TracInnovations, Ballerup, Denmark) used for retrospective motion correction of positron emission tomography scans[38,39] and prospective real-time motion correction of MR imaging scans.[39,40] A more detailed description of the Tracoline system is provided in Figure S1. A representative recording of a participant's absolute 3D motion is displayed in Figure 2. From this 3D motion recording, two 3D motion parameters were calculated (Figure 2): (1) the 3D motion standard deviation (3D SD) during the ^{1}H-MRS scan, representing an estimate for head motion variability and (2) the difference in 3D motion (3D DIFF) from the beginning to the end of the ^{1}H-MRS scan, representing an estimate of the mean head displacement.

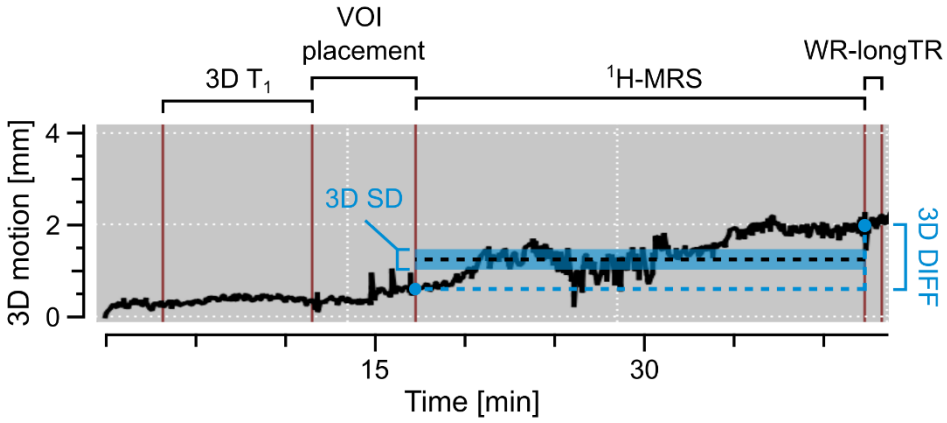

Figure 2. Representative absolute 3D motion recording. The two calculated 3D motion parameters are visually represented in blue: 3D motion standard deviation (3D SD) as estimate for head motion variability and (2) the difference in 3D motion (3D DIFF) as estimate of the mean head displacement. The beginning and the end of the proton magnetic resonance spectroscopy (^{1}H-MRS) acquisition in the periaqueductal grey (PAG) was manually labelled during the scan (red lines) within the TracSuite software. 3D T_1: anatomical T_1-weighted scan; VOI: volume of interest; WR-longTR: water reference scan with a long repetition time.

2.4 Statistical analysis

All statistical analyses were performed using RStudio for Mac (2022.12.0+353). Statistical significance was set at α=0.05 with a false discovery rate (FDR) correction per tested research question. The number of corrected tests per research question is indicated as N-FDR.

Normal distribution was assessed via inspection of histograms and QQ-plots. Because the majority of investigated outcome measures was not normally distributed, all values are reported as median (interquartile range) and all statistical analyses were performed using non-parametric tests.

SNR and FWHM of the NAA peak (FWHM NAA; post-processing quality indicator), as well as absolute Cramér-Rao lower bounds (CRLB) (relative CRLBs corrected for the metabolite concentration[41]) for the metabolites tCre (Cre + phosphocreatine), tCho (glycerophospho-choline + phosphocholine), tmI (mI + glycine), tNAA (NAA + N-acetylaspartylglutamate), pooled levels of Glu + Glutamine (Glx), and GABA, were compared between spectra processed with spectral registration and spectra processed without spectral registration using Pratt signed-rank tests (an alternative for Wilcoxon signed-rank tests accounting for ties[42]) (N-FDR=8).

To investigate whether spectral registration was particularly useful in cases of greater head motion, relative improvements in SNR and FWHM NAA were correlated with head motion variability (3D SD) and mean head displacement (3D DIFF) using Spearman correlations (N-FDR=4).

Metabolite concentrations of tCre, tCho, tmI, tNAA, Glx and GABA were compared between the literature-based and the individual-based metabolite quantification approach, i.e. using the water signal from the WR-shortTR scan and using the water signal from the WR-longTR scan, respectively, using Pratt signed-rank tests (N-FDR=6).

For Pratt signed-rank tests, effect sizes are reported as r (small effect: 0.1-<0.3, medium effect: 0.3-<0.5, large effect: ≥0.5 large effect[43]).

3. Results

3.1 Participant demographics

Out of the 35 recruited participants, one was excluded due to a suspected neurological disorder and one discontinued the scanning session due to discomfort. This resulted in a sample of 33 participants (mean age of 50.1 years, SD=17.19, 18 females) in whom ^{1}H-MRS was performed.

For spectra processed with spectral registration and spectra processed without spectral registration, visual inspection led to the exclusion of the same three participants (Figure S2). No participant presented with FWHM H_2O above or SNR values below 2.5 MAD of the sample median.

3.2 Improved spectral quality with spectral registration

A representative single spectrum and overlaid single spectra together with the group average for both post-processing approaches are shown in Figure 3. The FWHM H_2O reflecting the quality of the shim was 5.4 Hz (4.88-5.62) (Figure 4A).

Spectral registration significantly improved the SNR (Z=2.26, *p*=0.048, r=0.41), FWHM NAA (Z=-4.72, *p*<0.001, r=0.86), and absolute CRLBs of all investigated metabolites (Z's<-2.22, *p*'s<0.046, r's>0.41) of the acquired spectra (Table 1, Figure 4B).

Less improvement in spectral quality with greater head motion

On average, participants showed a head motion variability (3D SD) of 0.5 mm (0.32-0.73) and a mean head displacement (3D DIFF) of 1.7 mm (0.62-2.64) during the ^{1}H-MRS scan.

Greater mean head displacement (3D DIFF; rho=-0.58, *p*=0.002) but not head motion variability (3D SD; rho=-0.31, *p*=0.400) was associated with less relative improvement in SNR (Figure S3). Relative improvement in FWHM NAA was not associated with head motion measures (rho's <0.3, *p*'s >0.400).

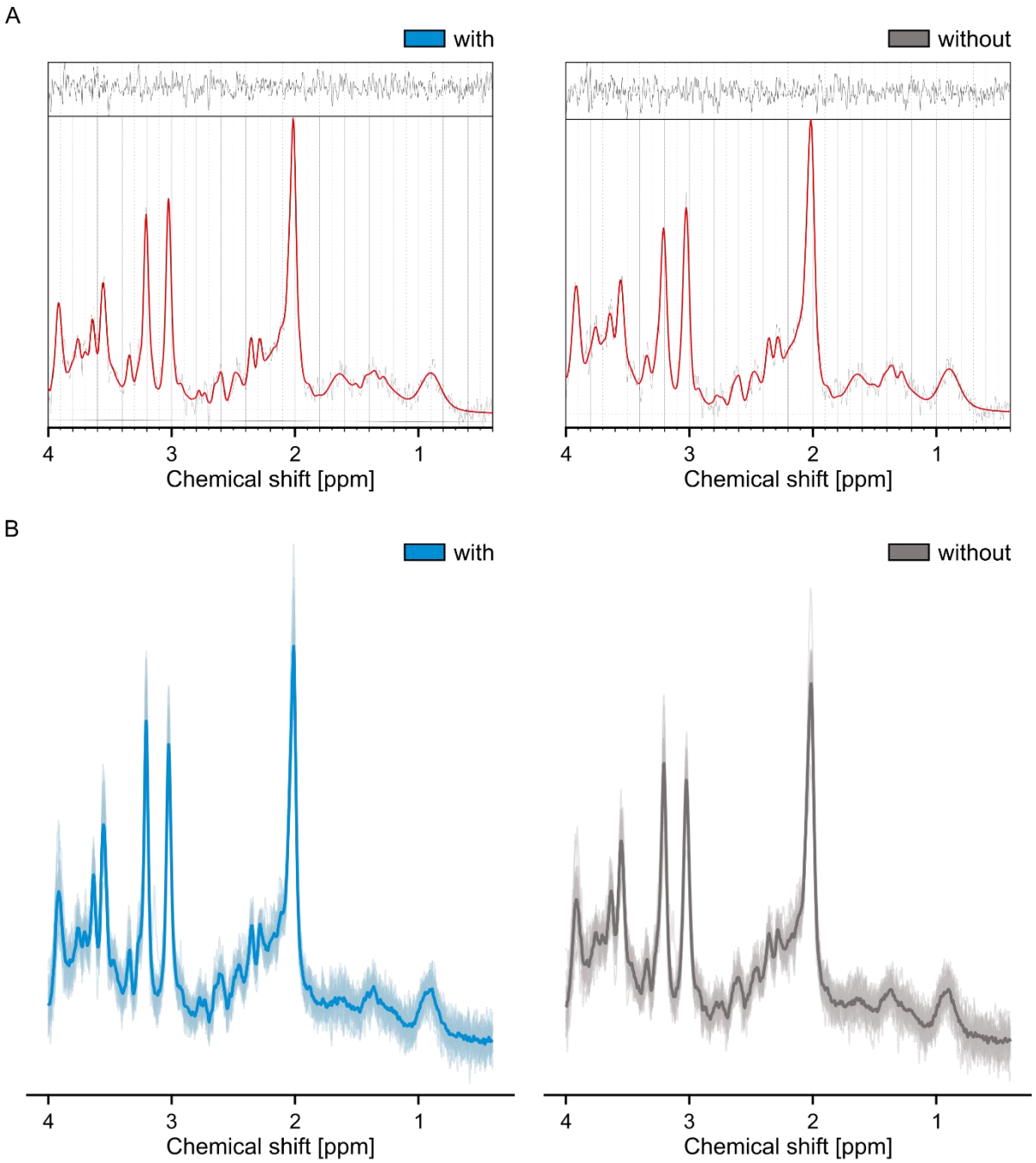

Figure 3. Spectra processed with and without spectral registration. Representative single spectra shown in (A) are from the same individual who showed a median signal-to-noise ratio (SNR), i.e. 18, in both post-processing approaches. Spectra were acquired using a point-resolved spectroscopy sequence optimized with very selective saturation pulses (OVERPRESS) and voxel-based flip angle calibration (TR: 2500 ms, TE: 33 ms, number of signals averaged: 512 divided into 8 blocks of 64, volume of interest size: 8.8x10.2x12.2 mm^3=1.1 mL).

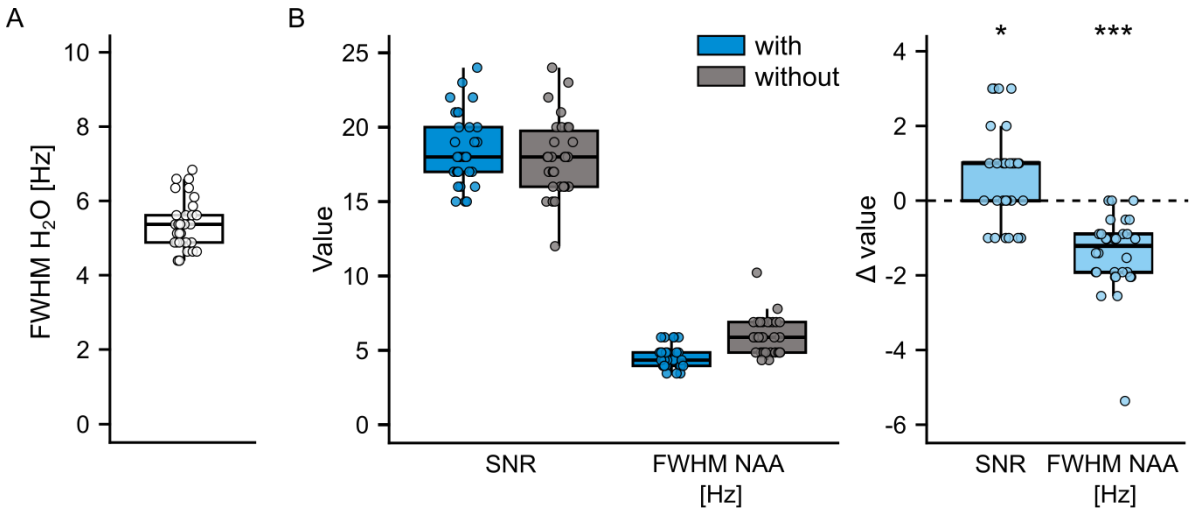

Figure 4. Improved spectral quality with spectral registration. Full width at half maximum values of the water peak (FWHM H_2O) (A) reflect the quality of the shim and apply to both post-processing approaches. Differences (Δ) in SNR and full width at half maximum values of the N-acetylaspartate peak (FWHM NAA) were calculated by subtracting the values obtained without spectral registration from the values obtained with spectral registration. An improvement using spectral registration is reflected in positive differences for SNR and in negative differences for FWHM NAA. * $p<0.05$, *** $p<0.001$.

3.3 Higher metabolite concentrations using individual-based quantification approach

Metabolite quantification using the subject-specific water signal from the WR-longTR scan, i.e. the individual-based quantification approach, yielded higher concentrations for all investigated metabolites (Z's >4.29, *p*'s<0.001, r's>0.78) compared to the literature-based approach using the water signal from the WR-longTR scan (Table 1, Figure 5).

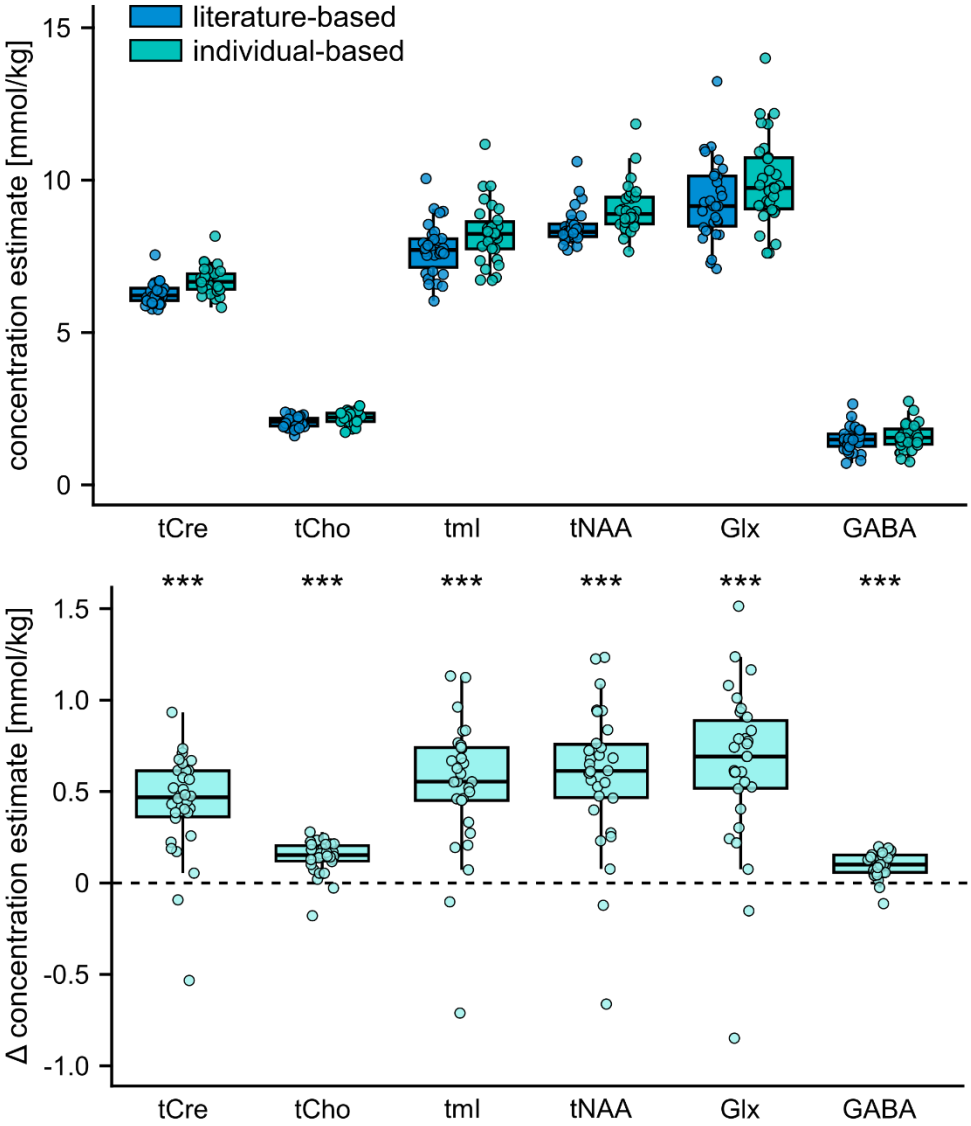

Figure 5. Higher metabolite concentrations using individual-based water relaxation times. Differences (Δ) in metabolite concentration estimates were calculated by subtracting the values obtained with literature-based water relaxation times from the values obtained with individual-based water relaxation times. Positive differences reflect higher metabolite concentrations individual-based water relaxation times. *** $p<0.001$. GABA: γ-aminobutyric acid; Glx: glutamate + glutamine; tCho: glycerophosphocholine + phosphocholine; tCre: creatine + phosphocreatine; tmI: myo-inositol + glycine; tNAA: N-acetylaspartate + N-acetylaspartylglutamate.

4. Discussion and Conclusions

This study aimed to record high-quality ^{1}H-MR spectra with optimized regional specificity in the brainstem PAG. Spectral registration[20] was used to address the challenge of increased frequency drifts and phase errors during the prolonged ^{1}H-MRS acquisition needed for the

small VOI size of 8.8x10.2x12.2 mm^3. Using spectral registration, all quality measures of the acquired spectra improved, resulting in high spectral quality in the methodologically challenging PAG.

Compared to previous PAG ^{1}H-MRS studies,[12-15] this study's approach allowed higher regional specificity together with quantification of neurobiologically relevant metabolites detected at short TEs such as Glx. Because these previous studies did not report spectral quality measures, a direct quality comparison is not possible. However, the here achieved spectral quality is comparable or even superior to studies which examined other brainstem VOIs of larger size[44-49] and superior to one study with a brainstem VOI of similar size.[50] Regarding GABA, PRESS sequences have limitations because GABA's signal overlaps with resonances from other metabolites and is therefore difficult to detect. Other techniques allow a more reliable GABA detection, such as the MEscher-GArwood (MEGA) PRESS.[51] Yet, MEGA-PRESS is highly susceptible to frequency drifts[52] and requires VOI sizes of approximately 30x30x30 mm^3, making it unsuitable for the PAG. Moreover, the CRLBs for GABA of the present study (median absolute: 62.44 I.U., median relative: 24 %) indicate an adequate reliability of the concentration measurement and the detected concentrations lie within the expected range for human brain tissue.[53] A disadvantage of the sequence used here is the prolonged scan duration, which might be particularly challenging for patient cohorts. Advances in MR methodology, e.g. higher field strengths, might allow to achieve similar spectral quality with shorter scan durations. Nevertheless, the presented technique offers new opportunities to investigate PAG function and might translate to other clinically relevant small-sized brain regions prone to physiological noise, such as the hippocampus.

Head motion is a source for frequency and phase errors.[20,21] Because spectral registration corrects for frequency and phase errors,[20] it might be particularly useful in cases of greater head motion. Interestingly, the opposite was observed, i.e. the more participants moved during the ^{1}H-MRS scan, the smaller the SNR improvement. Potential reasons for this observation were examined by exploring how spectral quality improvement and head motion were associated with measured frequency drifts and phase errors. It was observed that (1) spectral registration mainly improved SNR for spectra with larger frequency fluctuations but not phase fluctuations, and (2) larger phase fluctuations were associated with smaller FWHM NAA improvement (Figure S4). Thus, in the present study, spectral registration corrected for frequency errors while phase errors impeded effective spectral registration. Head motion did not correlate with frequency drifts or phase errors, but previous studies have shown that translational head motion leads to phase shifts while frequency changes in response to small head movements may be negligible.[21] Taken together, head motion might have induced phase

errors which spectral registration was not able to account for, resulting in negative effects on spectral quality improvement. Of note, the here used motion tracking system is based on 3D surface tracking, which cannot be directly translated to the actual displacement of the PAG. Nevertheless, the markerless motion tracking system allows simple real-time motion monitoring which might help decisions on whether a sequence should be repeated due to excessive head motion.

The current gold-standard for metabolite quantification is referencing the metabolite signal to the water signal from the same VOI corrected for partial volume and tissue-specific relaxation effects.[54] Literature provides reference values for the therefore required tissue-specific water T_1/T_2 relaxation times, but these might not generalize to the PAG because T_1/T_2 relaxation times vary across different brain regions.[30-32] Therefore, metabolite concentrations were not only quantified using literature-based (WR-shortTR) but also individual-based (WR-longTR) water relaxation times. Using the individual-based approach, 7.5% higher metabolite concentrations were estimated compared to the literature-based approach meaning that the estimated water signal was smaller when individual-based water relaxation times were used. This effect is most likely due to T_1 relaxation time differences between the two approaches, because the here used literature-based T_2 relaxation times were similar to the T_2 values estimated via the TE series in the WR-longTR scan (81.25 ms [77.75-84.2]). This result raises the question whether the standard T_1 relaxation times apply to the PAG. Regardless, the "absolute" metabolite concentrations reported are valuable in that they allow comparison to future PAG ^{1}H-MRS studies.

In summary, spectral registration enabled the acquisition of high-quality ^{1}H-MR spectra in the PAG, a physiologically and clinically highly relevant brainstem region. This approach offers the opportunity to further investigate the PAG's neurochemical properties in health and disease and might not only be applicable in the PAG, but also in other brain regions with similar methodological challenges.

Data availability

Data will be made available upon request for participants who gave informed consent on further use of their anonymized data.

Acknowledgments

This study was funded by the Clinical Research Priority Program "Pain" of the University of Zurich. L. Sirucek is supported by the Theodor und Ida Herzog-Egli Stiftung. The authors express their gratitude to Emma Louise Kessler, MD for her generous donation to the Zurich Institute of Forensic Medicine, University of Zurich, Switzerland.

References

1. Benarroch EE. Periaqueductal gray: an interface for behavioral control. Neurology 2012;78(3):210-217.
2. Zhou J, Greicius MD, Gennatas ED et al. Divergent network connectivity changes in behavioural variant frontotemporal dementia and Alzheimer's disease. Brain 2010;133(Pt 5):1352-1367.
3. Cole LJ, Gavrilescu M, Johnston LA et al. The impact of Alzheimer's disease on the functional connectivity between brain regions underlying pain perception. Eur J Pain 2011;15(6):568 e561-511.
4. Mainero C, Boshyan J, Hadjikhani N. Altered functional magnetic resonance imaging resting-state connectivity in periaqueductal gray networks in migraine. Ann Neurol 2011;70(5):838-845.
5. Li Z, Liu M, Lan L et al. Altered periaqueductal gray resting state functional connectivity in migraine and the modulation effect of treatment. Sci Rep 2016;6:20298.
6. Niu X, Bai L, Sun Y et al. Disruption of periaqueductal grey-default mode network functional connectivity predicts persistent post-traumatic headache in mild traumatic brain injury. J Neurol Neurosurg Psychiatry 2019;90(3):326-332.
7. Cifre I, Sitges C, Fraiman D et al. Disrupted functional connectivity of the pain network in fibromyalgia. Psychosom Med 2012;74(1):55-62.
8. Truini A, Tinelli E, Gerardi MC et al. Abnormal resting state functional connectivity of the periaqueductal grey in patients with fibromyalgia. Clin Exp Rheumatol 2016;34(2 Suppl 96):S129-133.
9. Harper DE, Ichesco E, Schrepf A et al. Resting Functional Connectivity of the Periaqueductal Gray Is Associated With Normal Inhibition and Pathological Facilitation in Conditioned Pain Modulation. J Pain 2018;19(6):635 e631-635 e615.
10. Mills EP, Di Pietro F, Alshelh Z et al. Brainstem Pain-Control Circuitry Connectivity in Chronic Neuropathic Pain. J Neurosci 2018;38(2):465-473.
11. Yu R, Gollub RL, Spaeth R et al. Disrupted functional connectivity of the periaqueductal gray in chronic low back pain. Neuroimage Clin 2014;6:100-108.

12. Lai TH, Fuh JL, Lirng JF, Lin CP, Wang SJ. Brainstem 1H-MR spectroscopy in episodic and chronic migraine. J Headache Pain 2012;13(8):645-651.
13. Wang W, Zhang X, Bai X et al. Gamma-aminobutyric acid and glutamate/glutamine levels in the dentate nucleus and periaqueductal gray with episodic and chronic migraine: a proton magnetic resonance spectroscopy study. J Headache Pain 2022;23(1):83.
14. Buonanotte F, Schurrer C, Carpinella M et al. [Alteration of the antinociceptive systems in chronic daily headaches]. Rev Neurol 2006;43(5):263-267.
15. Serrano-Munoz D, Galan-Arriero I, Avila-Martin G et al. Deficient Inhibitory Endogenous Pain Modulation Correlates With Periaqueductal Gray Matter Metabolites During Chronic Whiplash Injury. Clin J Pain 2019;35(8):668-677.
16. Duvernoy HM. The human brain stem and cerebellum: surface, structure, vascularization, and three-dimensional sectional anatomy, with MRI: Springer Science & Business Media; 1995.
17. Brooks JC, Faull OK, Pattinson KT, Jenkinson M. Physiological noise in brainstem FMRI. Front Hum Neurosci 2013;7:623.
18. Adam A, Dixon AK, Gillard JH. Grainger & Allison's Diagnostic Radiology: A Textbook of Medical Imaging: Elsevier; 2020.
19. Edelstein WA, Glover GH, Hardy CJ, Redington RW. The intrinsic signal-to-noise ratio in NMR imaging. Magn Reson Med 1986;3(4):604-618.
20. Near J, Edden R, Evans CJ et al. Frequency and phase drift correction of magnetic resonance spectroscopy data by spectral registration in the time domain. Magn Reson Med 2015;73(1):44-50.
21. Saleh MG, Edden RAE, Chang L, Ernst T. Motion correction in magnetic resonance spectroscopy. Magn Reson Med 2020;84(5):2312-2326.
22. Bottomley PA; Google Patents, assignee. Selective volume method for performing localized NMR spectroscopy. US Patent 4,480,228. October 30, 1984.
23. Ordidge R, Bendall M, Gordon R, Connelly A. Volume selection for in-vivo biological spectroscopy. Magnetic resonance in biology and medicine 1985:387-397.
24. Edden RA, Schar M, Hillis AE, Barker PB. Optimized detection of lactate at high fields using inner volume saturation. Magn Reson Med 2006;56(4):912-917.
25. Schulte RF, Henning A, Tsao J, Boesiger P, Pruessmann KP. Design of broadband RF pulses with polynomial-phase response. J Magn Reson 2007;186(2):167-175.
26. Wilson M, Andronesi O, Barker PB et al. Methodological consensus on clinical proton MRS of the brain: Review and recommendations. Magn Reson Med 2019;82(2):527-550.

27. Deelchand DK, Kantarci K, Oz G. Improved localization, spectral quality, and repeatability with advanced MRS methodology in the clinical setting. Magn Reson Med 2018;79(3):1241-1250.
28. Oz G, Deelchand DK, Wijnen JP et al. Advanced single voxel (1) H magnetic resonance spectroscopy techniques in humans: Experts' consensus recommendations. NMR Biomed 2020:e4236.
29. Olesen OV, Wilm J, Kouwe AVd et al. An MRI Compatible Surface Scanner. In Proceedings of the 22nd Annual Meeting of ISMRM, Milan, Italy; 2014. Abstract 1303.
30. Wright PJ, Mougin OE, Totman JJ et al. Water proton T1 measurements in brain tissue at 7, 3, and 1.5 T using IR-EPI, IR-TSE, and MPRAGE: results and optimization. MAGMA 2008;21(1-2):121-130.
31. Mejia AF, Sweeney EM, Dewey B et al. Statistical estimation of T1 relaxation times using conventional magnetic resonance imaging. Neuroimage 2016;133:176-188.
32. Thaler C, Hartramph I, Stellmann JP et al. T1 Relaxation Times in the Cortex and Thalamus Are Associated With Working Memory and Information Processing Speed in Patients With Multiple Sclerosis. Front Neurol 2021;12:789812.
33. Simpson R, Devenyi GA, Jezzard P, Hennessy TJ, Near J. Advanced processing and simulation of MRS data using the FID appliance (FID-A)-An open source, MATLAB-based toolkit. Magn Reson Med 2017;77(1):23-33.
34. Klose U. In vivo proton spectroscopy in presence of eddy currents. Magn Reson Med 1990;14(1):26-30.
35. Leys C, Ley C, Klein O, Bernard P, Licata L. Detecting outliers: Do not use standard deviation around the mean, use absolute deviation around the median. Journal of Experimental Social Psychology 2013;49:764-766.
36. Provencher SW. Estimation of metabolite concentrations from localized in vivo proton NMR spectra. Magn Reson Med 1993;30(6):672-679.
37. Kreis R, Ernst T, Ross BD. Absolute Quantitation of Water and Metabolites in the Human Brain. II. Metabolite Concentrations. Journal of Magnetic Resonance, Series B 1993;102(1):9-19.
38. Olesen OV, Sullivan JM, Mulnix T et al. List-mode PET motion correction using markerless head tracking: proof-of-concept with scans of human subject. IEEE Trans Med Imaging 2013;32(2):200-209.
39. Slipsager JM, Ellegaard AH, Glimberg SL et al. Markerless motion tracking and correction for PET, MRI, and simultaneous PET/MRI. PLoS One 2019;14(4):e0215524.

40. Benjaminsen C, Jensen RR, Wighton P et al. Real Time MRI Motion Correction with Markerless Tracking. In: Proceedings of the 24th Annual Meeting of ISMRM 2016;(abstract 1860).
41. Kreis R. The trouble with quality filtering based on relative Cramer-Rao lower bounds. Magn Reson Med 2016;75(1):15-18.
42. Pratt JW. Remarks on Zeros and Ties in the Wilcoxon Signed Rank Procedures. Journal of the American Statistical Association 1959;54(287):655-667.
43. Cohen J. A power primer. Psychol Bull 1992;112(1):155-159.
44. Oz G, Hutter D, Tkac I et al. Neurochemical alterations in spinocerebellar ataxia type 1 and their correlations with clinical status. Mov Disord 2010;25(9):1253-1261.
45. Oz G, Tkac I. Short-echo, single-shot, full-intensity proton magnetic resonance spectroscopy for neurochemical profiling at 4 T: validation in the cerebellum and brainstem. Magn Reson Med 2011;65(4):901-910.
46. Deelchand DK, Adanyeguh IM, Emir UE et al. Two-site reproducibility of cerebellar and brainstem neurochemical profiles with short-echo, single-voxel MRS at 3T. Magn Reson Med 2015;73(5):1718-1725.
47. de Matos NMP, Hock A, Wyss M, Ettlin DA, Brugger M. Neurochemical dynamics of acute orofacial pain in the human trigeminal brainstem nuclear complex. Neuroimage 2017;162:162-172.
48. Younis S, Hougaard A, Christensen CE et al. Effects of sildenafil and calcitonin gene-related peptide on brainstem glutamate levels: a pharmacological proton magnetic resonance spectroscopy study at 3.0 T. J Headache Pain 2018;19(1):44.
49. Younis S, Hougaard A, Christensen CE et al. Interictal pontine metabolism in migraine without aura patients: A 3 Tesla proton magnetic resonance spectroscopy study. Neuroimage Clin 2021;32:102824.
50. Emir UE, Tuite PJ, Oz G. Elevated pontine and putamenal GABA levels in mild-moderate Parkinson disease detected by 7 tesla proton MRS. PLoS One 2012;7(1):e30918.
51. Mescher M, Merkle H, Kirsch J, Garwood M, Gruetter R. Simultaneous in vivo spectral editing and water suppression. NMR in Biomedicine 1998;11(6):266-272.
52. Harris AD, Glaubitz B, Near J et al. Impact of frequency drift on gamma-aminobutyric acid-edited MR spectroscopy. Magn Reson Med 2014;72(4):941-948.
53. Govindaraju V, Young K, Maudsley AA. Proton NMR chemical shifts and coupling constants for brain metabolites. NMR Biomed 2000;13(3):129-153.
54. Near J, Harris AD, Juchem C et al. Preprocessing, analysis and quantification in single-voxel magnetic resonance spectroscopy: experts' consensus recommendations. NMR Biomed 2021;34(5):e4257.

Tables

Table 1. Quality measures and metabolite concentrations for ^{1}H-MRS spectra acquired in the PAG.

Measure	with spectral registration	without spectral registration	difference	difference [%]	Z	*p*	effect size r
SNR	18.0 (17.00-20.00)	18.0 (16.00-19.75)	1.0 (0.00-1.00)	4.8 (0.00-6.25)	2.26	0.048	0.41
FWHM NAA [Hz]	4.3 (3.96-4.85)	5.9 (4.85-6.90)	-1.2 (-1.92--0.90)	-22.6 (-29.63--14.81)	-4.72	<0.001	0.86
CRLB tCre [I.U.]	22.6 (21.78-24.50)	23.0 (22.08-30.80)	-0.3 (-0.67-0.12)	-1.3 (-3.10-0.57)	-2.22	0.026	0.41
CRLB tCho [I.U.]	9.9 (7.72-10.93)	10.7 (9.38-11.85)	-0.2 (-0.92--0.09)	-2.5 (-7.5--0.89)	-3.96	<0.001	0.72
CRLB tmI [I.U.]	38.0 (31.33-41.37)	39.9 (34.72-43.05)	-0.4 (-1.03--0.14)	-1.3 (-2.82--0.43)	-2.49	0.038	0.45
CRLB tNAA [I.U.]	29.5 (28.42-30.60)	30.0 (28.54-32.11)	-0.4 (-0.62-0.08)	-1.3 (-2.10-0.24)	-2.72	0.033	0.50
CRLB Glx [I.U.]	83.6 (77.84-89.25)	85.5 (81.34-94.10)	-4.1 (-6.62-0.32)	-4.7 (-6.83-0.37)	-2.53	0.046	0.46
CRLB GABA [I.U.]	62.44 (52.29-66.35)	72.47 (64.11-77.51)	-10.4 (-14.00--3.93)	-14.7 (-19.18--6.50)	-4.77	<0.001	0.87
CRLB tCre [%]	2 (2-2)	2 (2-3)					
CRLB tCho [%]	3 (2-3)	3 (3-3)					
CRLB tmI [%]	3 (2-3)	3 (3-3)					
CRLB tNAA [%]	2 (2-2)	2 (2-2)					
CRLB Glx [%]	5 (5-6)	5 (5-6)					
CRLB GABA [%]	24 (20-27)	21.5 (17.25-28.75)					

	WR-shortTR water signal	WR-longTR water signal	difference	difference [%]	Z	*p*	effect size r
tCre [mmol/kg]	6.2 (6.05-6.45)	6.7 (6.42-6.93)	0.5 (0.36-0.61)	7.5 (5.75-9.21)†	4.35	<0.001	0.79
tCho [mmol/kg]	2.1 (1.93-2.18)	2.2 (2.08-2.35)	0.2 (0.12-0.20)		4.35	<0.001	0.79
tmI [mmol/kg]	7.7 (7.14-8.07)	8.2 (7.74-8.64)	0.6 (0.45-0.74)		4.31	<0.001	0.79
tNAA [mmol/kg]	8.3 (8.15-8.56)	8.9 (8.56-9.44)	0.6 (0.47-0.76)		4.39	<0.001	0.80
Glx [mmol/kg]	9.2 (8.49-10.13)	9.7 (9.06-10.73)	0.7 (0.52-0.89)		4.29	<0.001	0.78
GABA [mmol/kg]	1.5 (1.26-1.67)	1.6 (1.33-1.83)	0.1 (0.06-0.15)		4.41	<0.001	0.81

Quality measures are reported for spectra with spectral registration and without spectral registration. Relative CRLBs are provided to help with interpretability but were not compared between the two postprocessing approaches because they are dependent on metabolite concentrations[41]. Absolute CRLBs were calculated by multiplying the relative CRLBs with the metabolite concentration as ratio to water from the LCModel output. Metabolite concentrations are reported for the metabolite quantification approach using the WR-shortTR water signal and the WR-longTR water signal. Values are reported as median (interquartile range). Relative differences in % were calculated as difference (with spectral registration – without spectral registration and WRlongTR – WR-shortTR) divided by the baseline value, i.e. quality measures of spectra processed without spectral registration or metabolite concentrations using the WR-shortTR water signal, respectively. Statistical comparisons were made using Pratt signed-rank tests[42]. *P*-values were false discovery rate corrected for N=8 tests (quality measures comparison) or N=6 tests (metabolite concentration comparison). Effect size interpretation: 0.1-<0.3, medium effect: 0.3-<0.5, large effect: ≥0.5 large effect[43]. CRLB: Cramér-Rao lower bound; FWHM: full width at half maximum; GABA: γ-aminobutyric acid; Glx: glutamate + glutamine; I.U.: institutional units; MRS: magnetic resonance spectroscopy; SNR: signal-to-noise ratio; tCho: glycerophosphocholine + phosphocholine; tCre: creatine + phosphocreatine; TE: echo time; tmI: myo-inositol + glycine; tNAA: N-acetylaspartate + N-acetylaspartylglutamate; TR: repetition time; VOI: volume of interest; WM: white matter. †The relative difference was identical for all metabolites because it was driven by differently estimated water signals which affected all metabolites to the same degree.